Temperature evolution in internally-heated packed-bed tanks for high-temperature solid-air energy storage: An asymptotic approach for an optimized design

A. Martín-Alcántara[1], R. Fernandez Feria[2]

[1]Mechanical Engineering, Universidad de Córdoba
[2]Fluid Mechanics, Universidad de Málaga

Motivation: Global Energy Challenge

Mean problem: Renewable energy intermittency → mismatch between generation and demand.

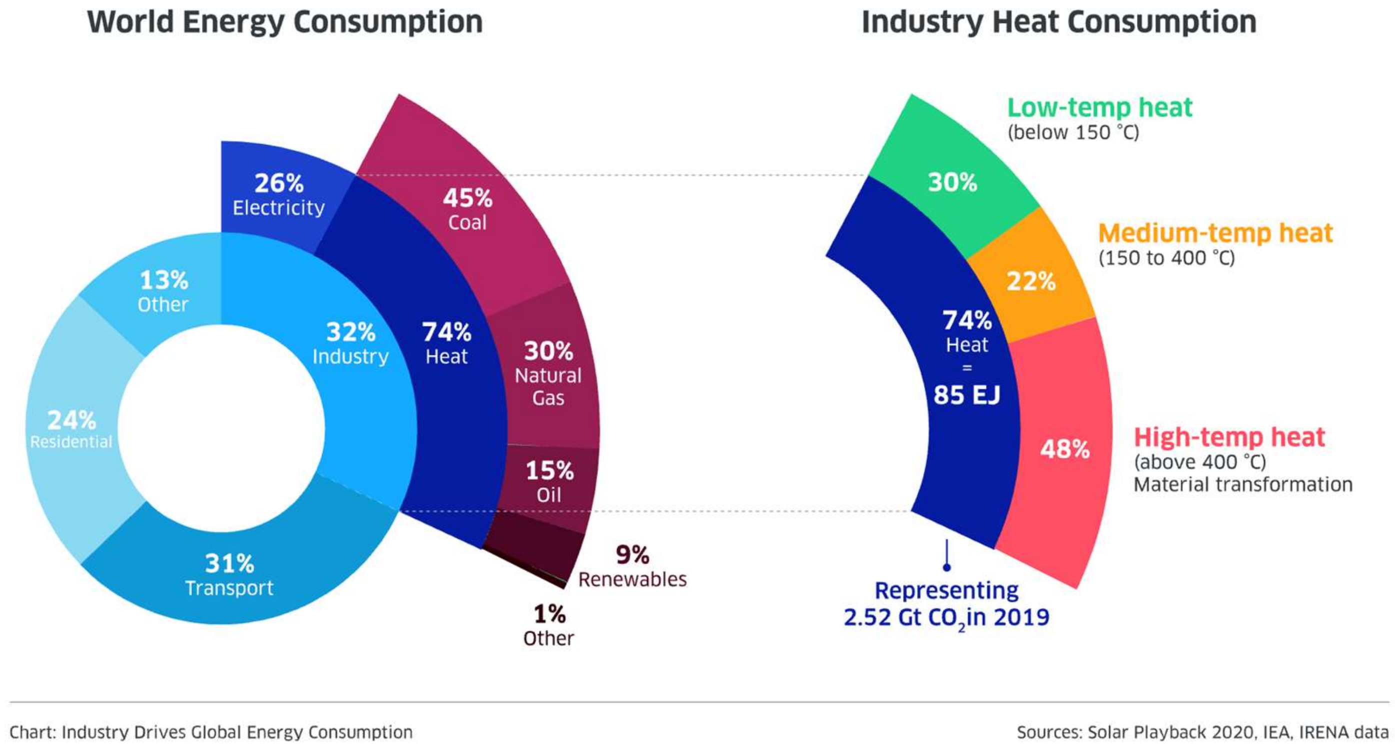

Motivation: Global Energy Challenge

- More focused on high-temperature industries (steel, chemicals, ceramics).

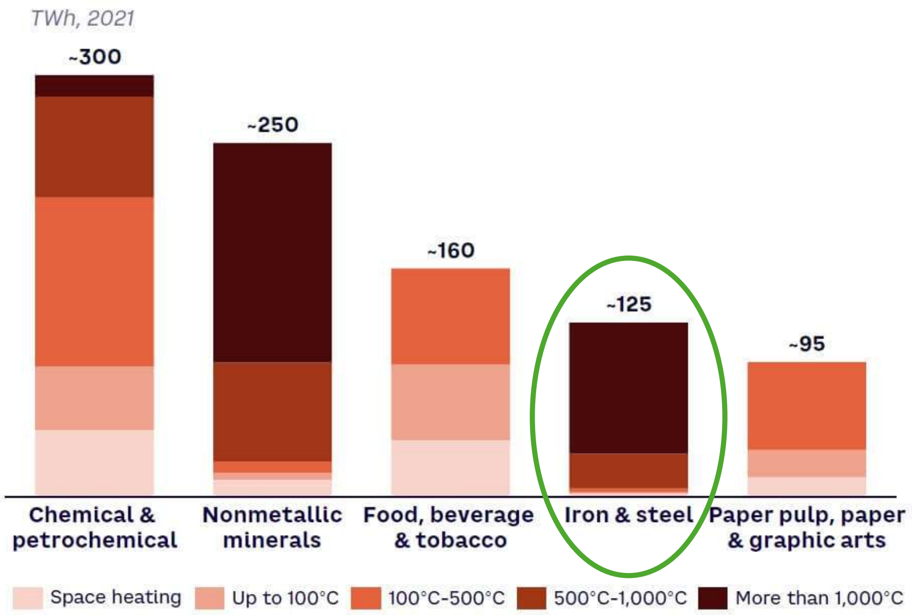

Source: Arthur D. Little

- Difficult to decarbonize: *hard-to-abate* sectors (European Green Deal).
- Goal: support 2050 net-zero targets.

Motivation: High-Temperature Packed-bed TES

- Stores sensible heat at T >800–1000 °C with cheap, solid fillers (rocks, concrete).
- PCM tanks not operating in this range.
- Air/Gas as HTF: no phase change, lower cost vs. lower efficiency.
- Well-studied (mostly numerical and experimentially).

- Cannot ensure outlet temperature -> need additional power.

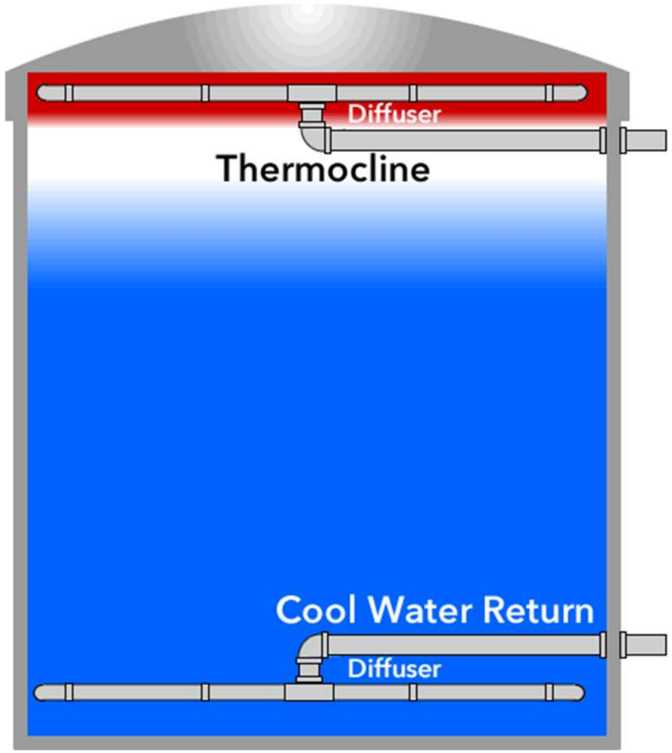

Source: Pacific Tank

Motivation. From Passive Storage to Active Heating

- Carnot Batteries: electricity → thermal storage (TES) → electricity.
- Heat to electricity: turbines, thermochemical.

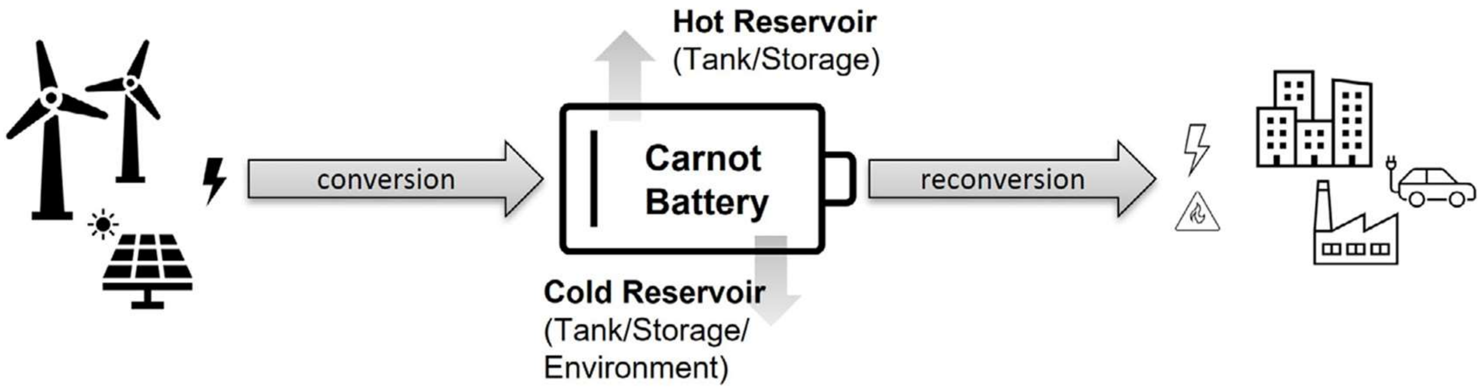

Source: Paul et al. (2022)

- Alternative: electricity → thermal storage (TES) → heat.
- All-in-one solution devoted to high-temperature industry.

Motivation. Existing internally-heated solutions (I)

- **FIRES** system uses longitudinal heat sources (suboptimal).

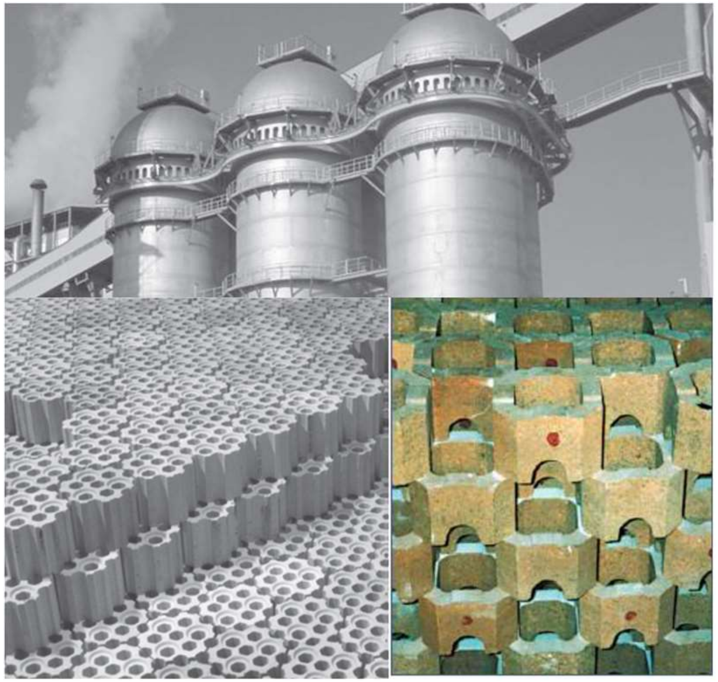

Source: Stack et al. (2019)

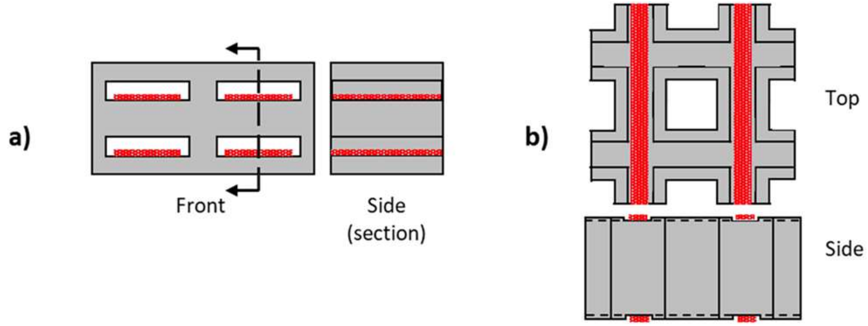

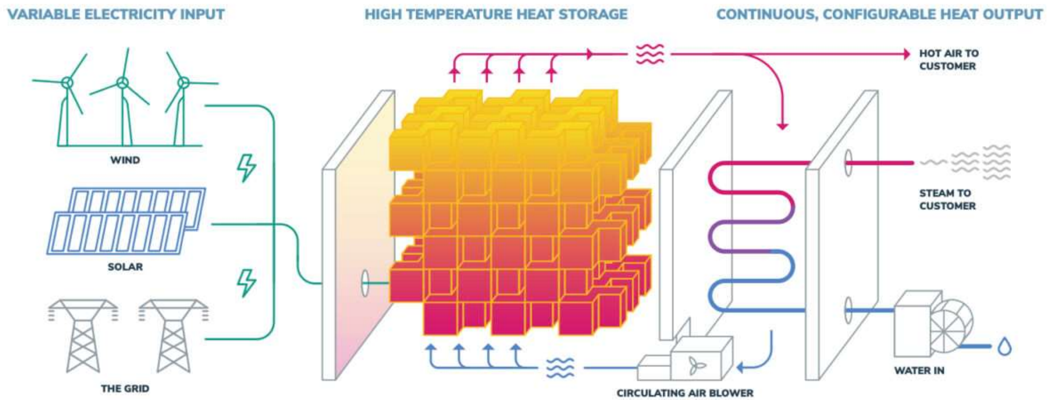

Source: https://pv-magazine-usa.com/

Motivation. Existing internally-heated solutions (II)

- **ANTORA**: electricity -> liquid tin -> TES -> thermophotovoltaics (40 % efficiency) -> electricity

ANTORA

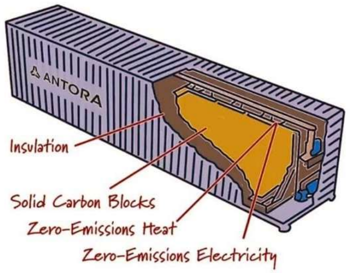

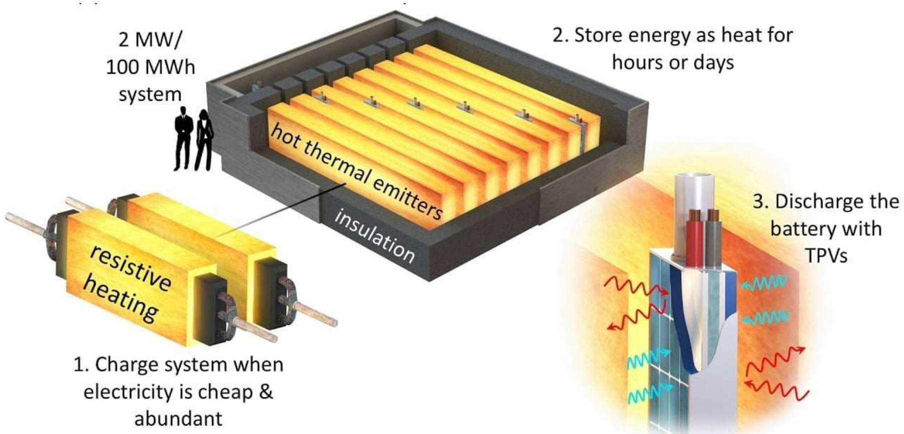

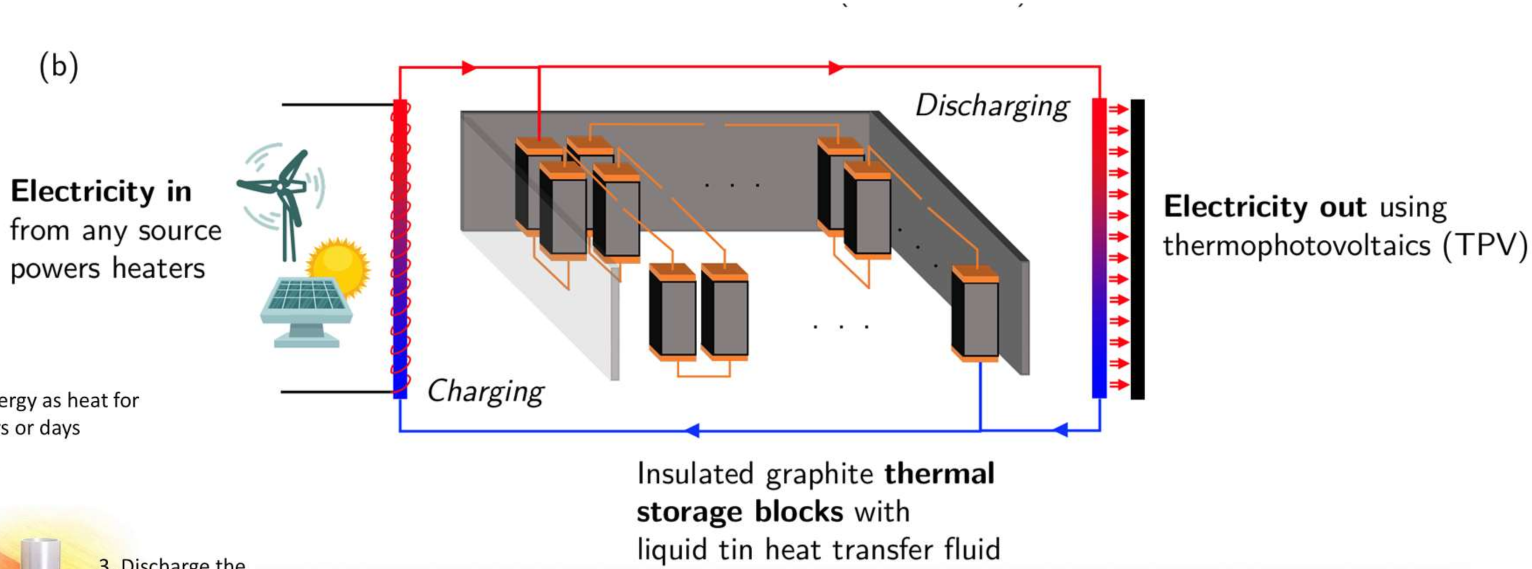

Source: Verma et al. (2024)

Motivation. Our concept: IH-TESLA

- Internally-Heated TES tank with Localized heat Application.
- Optimized heat transfer HTF <-> internal heat source.
- The flow receives all the power to meet a ref. outlet temperature.
- No need for control to ensure final needs.

- Mathematical model based on Schumann's.

HEAT TRANSFER: A LIQUID FLOWING THROUGH A POROUS PRISM.

BY

T. E. W. SCHUMANN,

Combustion Utilities Corporation,
Linden, N. J.

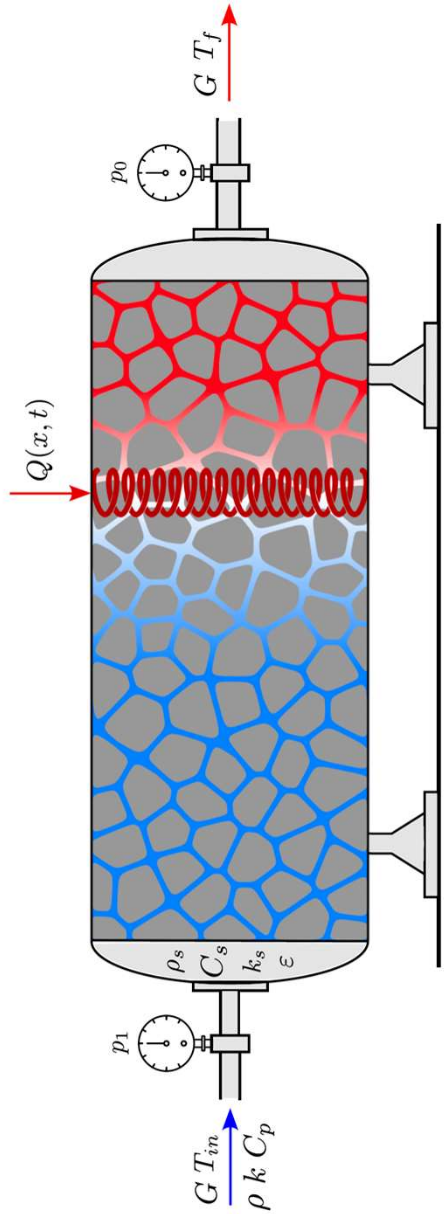

Source: Martín-Alcántara and Fernandez Feria (2025)

Motivation. IH-TESLA operation

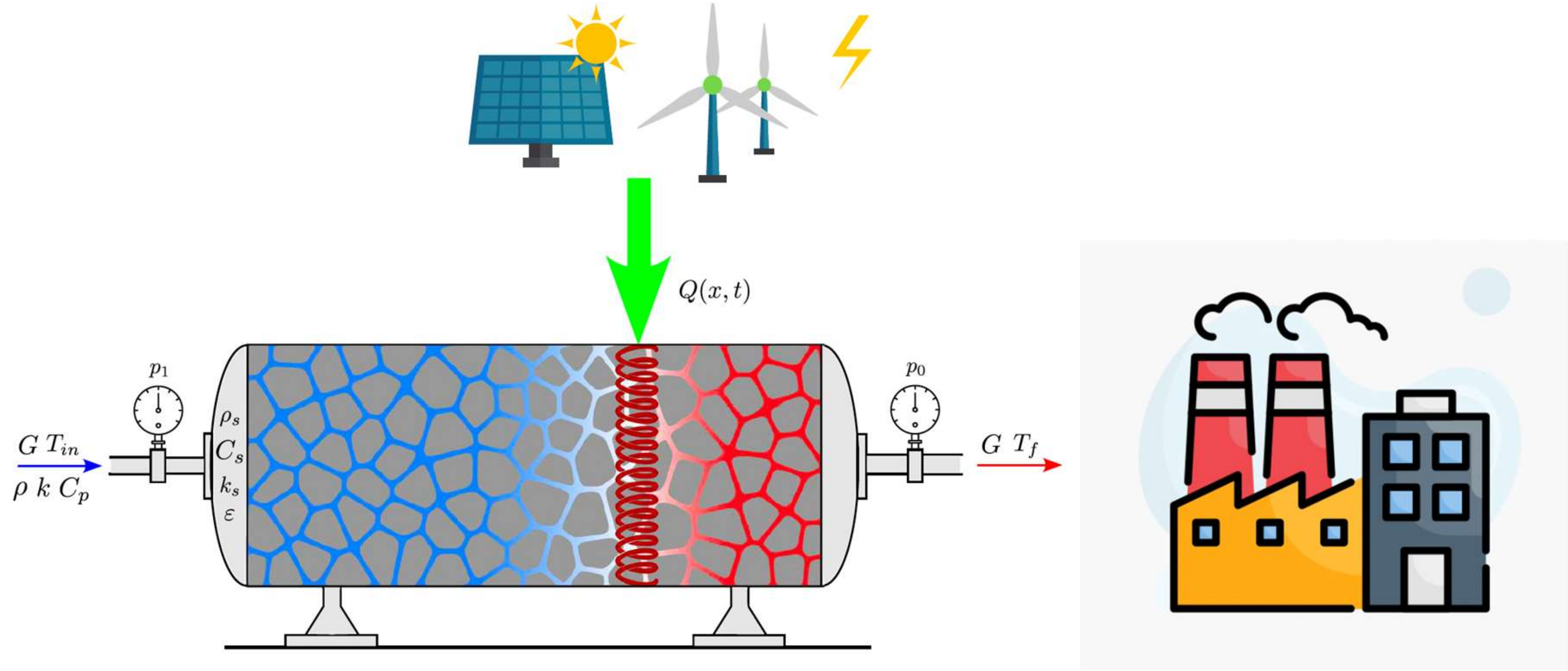

- Objective: Heat supply to a final user at a required temperature.

Mathematical formulation: Convective heat transfer in porous media

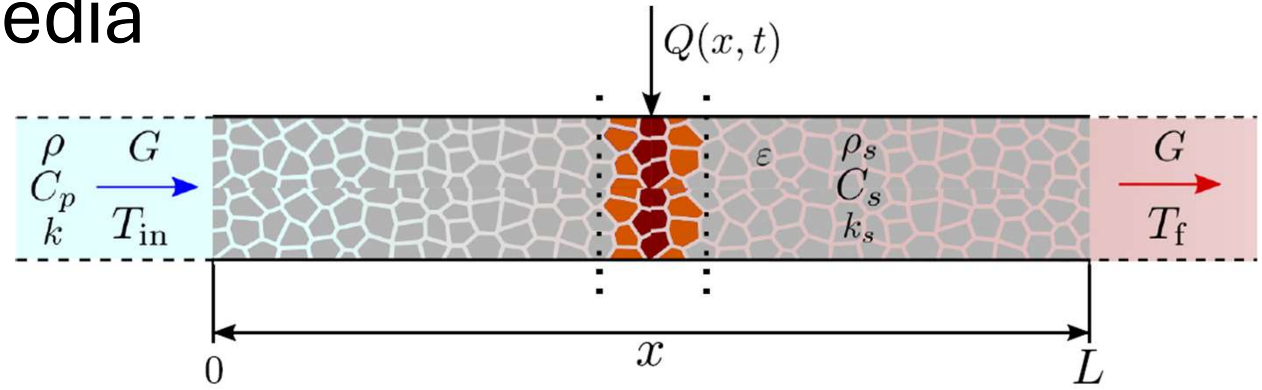

Source: Martín-Alcántara and Fernandez Feria (2025)

Governing Equations:

$$\varepsilon\rho C_p\left(\frac{\partial T}{\partial t}+u_0\frac{\partial T}{\partial x}\right)=\varepsilon k\frac{\partial^2 T}{\partial x^2}-h_v\left(T-T_s\right),$$

$$(1-\varepsilon)\rho_s C_s\frac{\partial T_s}{\partial t}=(1-\varepsilon)k_s\frac{\partial^2 T_s}{\partial x^2}+h_v\left(T-T_s\right)+Q(x,t),$$

Boundary and initial conditions:

$$T=T_{\mathrm{in}},\quad \frac{\partial T_s}{\partial x}=0,\quad \text{at } x=0,$$

$$\frac{\partial T}{\partial t}+u_0\frac{\partial T}{\partial x}=0,\quad \frac{\partial T_s}{\partial x}=0,\quad \text{at } x=L,$$

$$T(x)=T_s(x)=T_0,\qquad \text{at } t=0.$$

Mathematical formulation: Parameters and dimensionless expressions

Nondimensional formulation:

$$\tau = \frac{t\,u_0}{L}, \qquad \eta = \frac{x}{L},$$
$$\theta = \frac{T - T_0}{T_f - T_0}, \quad \theta_s = \frac{T_s - T_0}{T_f - T_0},$$

$$\gamma \frac{\partial \theta}{\partial \tau} + \frac{\partial \theta}{\partial \eta} = \beta \frac{\partial^2 \theta}{\partial \eta^2} - \Lambda\,(\theta - \theta_s)\,,$$
$$\frac{\partial \theta_s}{\partial \tau} = \frac{\kappa \beta}{\gamma} \frac{\partial^2 \theta_s}{\partial \eta^2} + \Lambda\,(\theta - \theta_s) + q(\eta, \tau)$$

$$0 \leq \eta \leq 1 \qquad 0 \leq \tau \leq 1$$

$$\theta = 0, \quad \frac{\partial \theta_s}{\partial \eta} = 0, \quad \text{at } \eta = 0,$$
$$\frac{\partial \theta}{\partial \tau} + \frac{\partial \theta}{\partial \eta} = 0, \quad \frac{\partial \theta_s}{\partial \eta} = 0, \quad \text{at } \eta = 1,$$
$$\theta = \theta_s = 0, \quad \text{at } \tau = 0.$$

Governing Parameters:

$$\Lambda = \frac{h_v L}{\varepsilon \rho\, C_p u_0}$$

Fluid-solid heat transfer

$$\kappa = \frac{\alpha_s}{\alpha}$$

Solid-to-fluid diffusivity ratio

$$\beta = \frac{k}{L u_0 \rho\, C_p}$$

Fluid conductivity

$$\gamma = \frac{\varepsilon \rho\, C_p}{(1-\varepsilon)\rho_s C_s}$$

Fluid-to-solid volumetric heat capacity

Problem dominated by:

$$\Lambda \gg 1$$
$$\kappa\,,\ \beta\,,\ \gamma \ll 1$$

HTF receiving all the heat:

$$\int_0^1 q_f(\eta)\mathrm{d}\eta = 1.$$

Internally localized heat source:

$$q(\eta, \tau) = \tanh\left(\frac{\tau}{\Delta_\tau}\right) \frac{\exp\left[-(\eta - \eta_1)^2/\Delta\right]}{\sqrt{\pi \Delta}}$$
$$q(\eta, \tau) = f(\tau) q_f(\eta)$$

Mathematical formulation. Scaling

Orders of magnitude of the parameters:

$$\kappa \sim \Lambda^{-1} \sim \epsilon\,, \quad \gamma \sim \beta \sim \epsilon^2\,, \qquad \epsilon \ll 1$$

$$\Lambda^{-1} \equiv \epsilon, \quad \frac{\kappa\beta}{\gamma} \equiv a\epsilon, \quad \beta \equiv b\epsilon^2, \quad \gamma \equiv c\epsilon^2$$

Estimation of *heating time*:

$$t_c = \frac{L}{u_0}\gamma^{-1} = \frac{(1-\varepsilon)\rho_s C_s L}{\varepsilon \rho C_p u_0}$$

Singular perturbation problem:

$$c\epsilon^3 \frac{\partial \theta}{\partial \tau} + \epsilon \frac{\partial \theta}{\partial \eta} = b\epsilon^3 \frac{\partial^2 \theta}{\partial \eta^2} - (\theta - \theta_s)\,,$$

$$\epsilon \frac{\partial \theta_s}{\partial \tau} = a\epsilon^2 \frac{\partial^2 \theta_s}{\partial \eta^2} + (\theta - \theta_s) + \epsilon\, q(\eta,\tau),$$

$$\theta = 0, \quad \frac{\partial \theta_s}{\partial \eta} = 0, \quad \text{at } \eta = 0,$$

$$\epsilon^2 \frac{\partial \theta}{\partial \tau} + \frac{\partial \theta}{\partial \eta} = 0, \quad \frac{\partial \theta_s}{\partial \eta} = 0, \quad \text{at } \eta = 1,$$

$$\theta = \theta_s = 0, \quad \text{at } \tau = 0.$$

Solution at each order:

$$\theta = \theta_0 + \epsilon\theta_1 + \epsilon^2\theta_2 + \dots,$$

$$\theta_s = \theta_{s0} + \epsilon\theta_{s1} + \epsilon^2\theta_{s2} + \dots.$$

$$O(1):\ \theta_0(\eta,\tau) = \theta_{s0}(\eta,\tau)$$

$$O(\epsilon):\ \theta_0(\eta,\tau) = \frac{1}{2}\left[\operatorname{erf}\left(\frac{\eta-\eta_1}{\sqrt{\Delta}}\right) + \operatorname{erf}\left(\frac{\tau-\eta+\eta_1}{\sqrt{\Delta}}\right)\right]$$

$$O(\epsilon^2):\ \theta_{s1}(\eta,\tau) = \frac{(a+1)}{\sqrt{\pi\Delta}}\left[e^{-(\eta-\eta_1)^2/\Delta} - 2e^{-(\eta-\tau-\eta_1)^2/\Delta} + e^{-(\eta-2\tau-\eta_1)^2/\Delta}\right]$$

$$\theta_1(\eta,\tau) = \frac{1}{\sqrt{\pi\Delta}}\left[a\, e^{-(\eta-\eta_1)^2/\Delta} - (2a+1)e^{-(\eta-\tau-\eta_1)^2/\Delta} + (a+1)e^{-(\eta-2\tau-\eta_1)^2/\Delta}\right]$$

Results. Theory validation with DNS

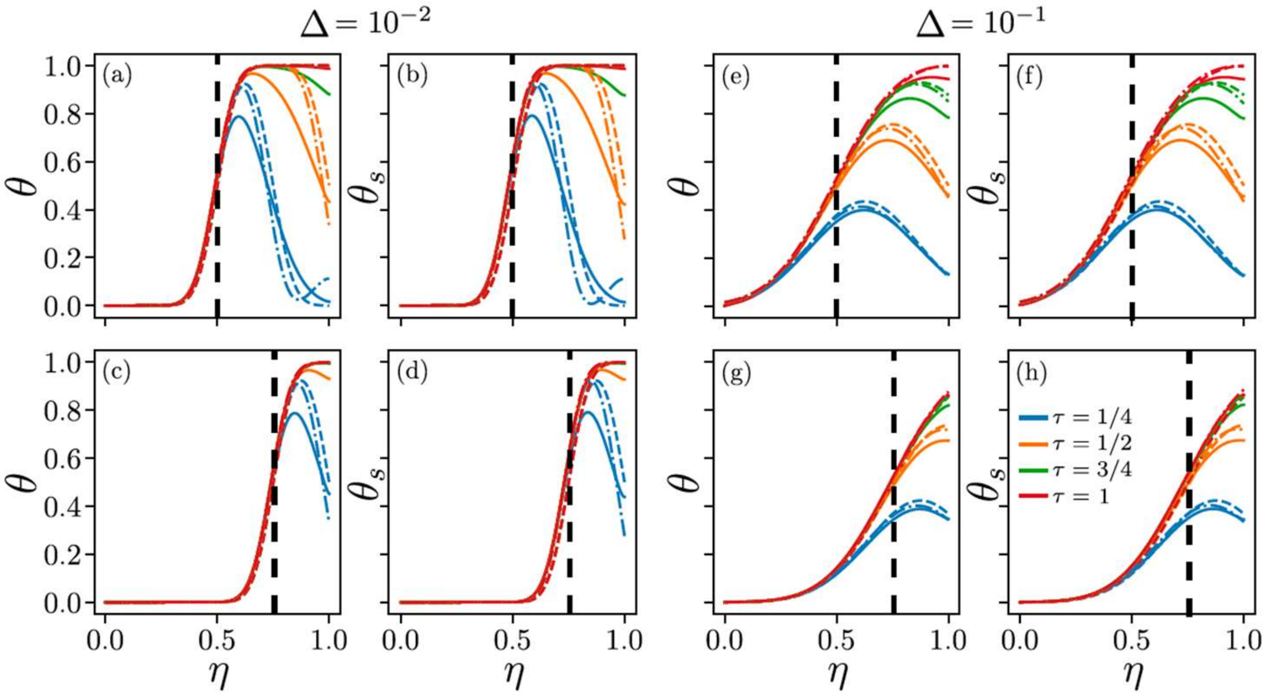

DNS (solid lines), zeroth- (dashed lines), and first-order (dash-dotted lines) asymptotic solutions for:

$\epsilon = \Lambda^{-1} = \kappa = 0.01$ and $\gamma = \beta = 10^{-4}$.

- Heat source thickness $\Delta = 10^{-1}$ not ensuring $\theta = 1$ at $\eta = 1$ for $\tau < 1$.
- Thickness of $\Delta = 10^{-2}$ meets the final needs, but with $\eta_1 = 3/4$, smaller θ decayment downstream the heat source.
- Solid temperature not surpassing that of the HTF with $\Delta = 10^{-2}$.

Results. Theory validation with DNS

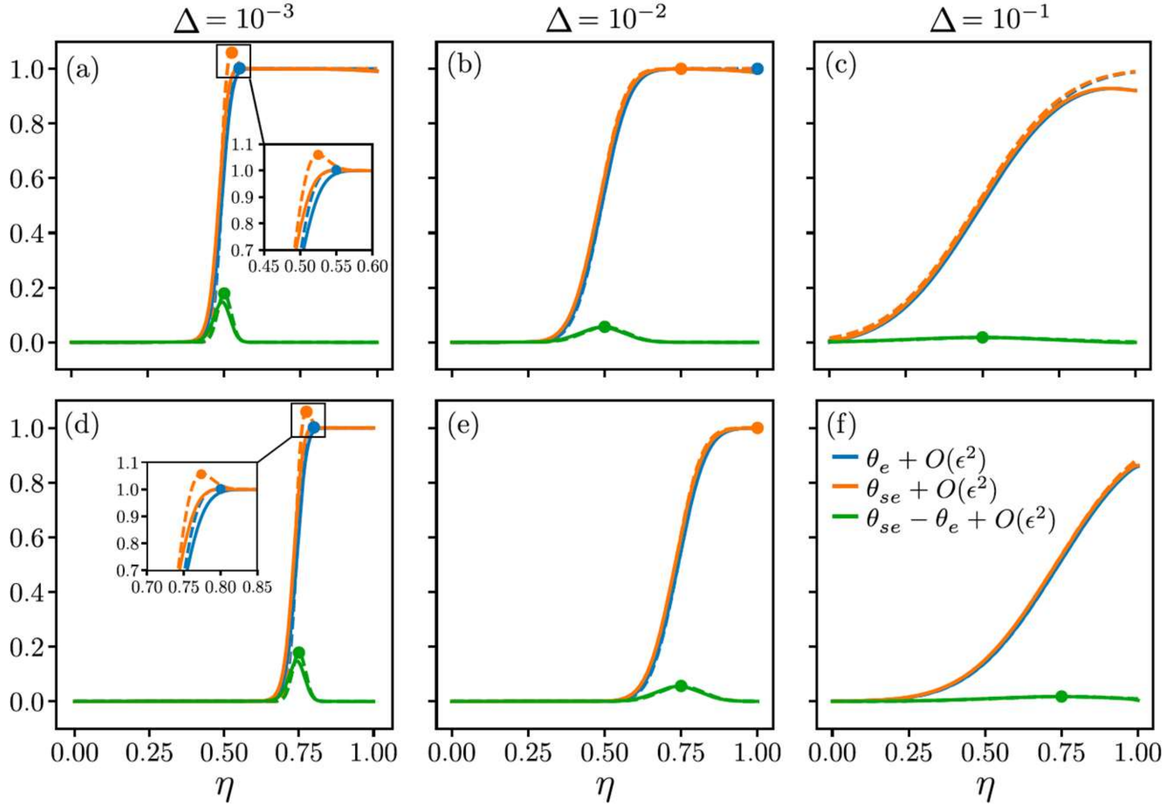

DNS (solid) and first-order (dashed) asymptotic solutions for the fluid (blue) and solid (orange) final temperatures, and for their differences (green).

$\epsilon = \Lambda^{-1} = \kappa = 0.01$ and $\gamma = \beta = 10^{-4}$.

- Solid temperature surpassing that of the HTF over $\Delta = 10^{-2}$.
- Thinner sources impractical and promotes overheating.

Results. Validation of 1D-flow hypothesis

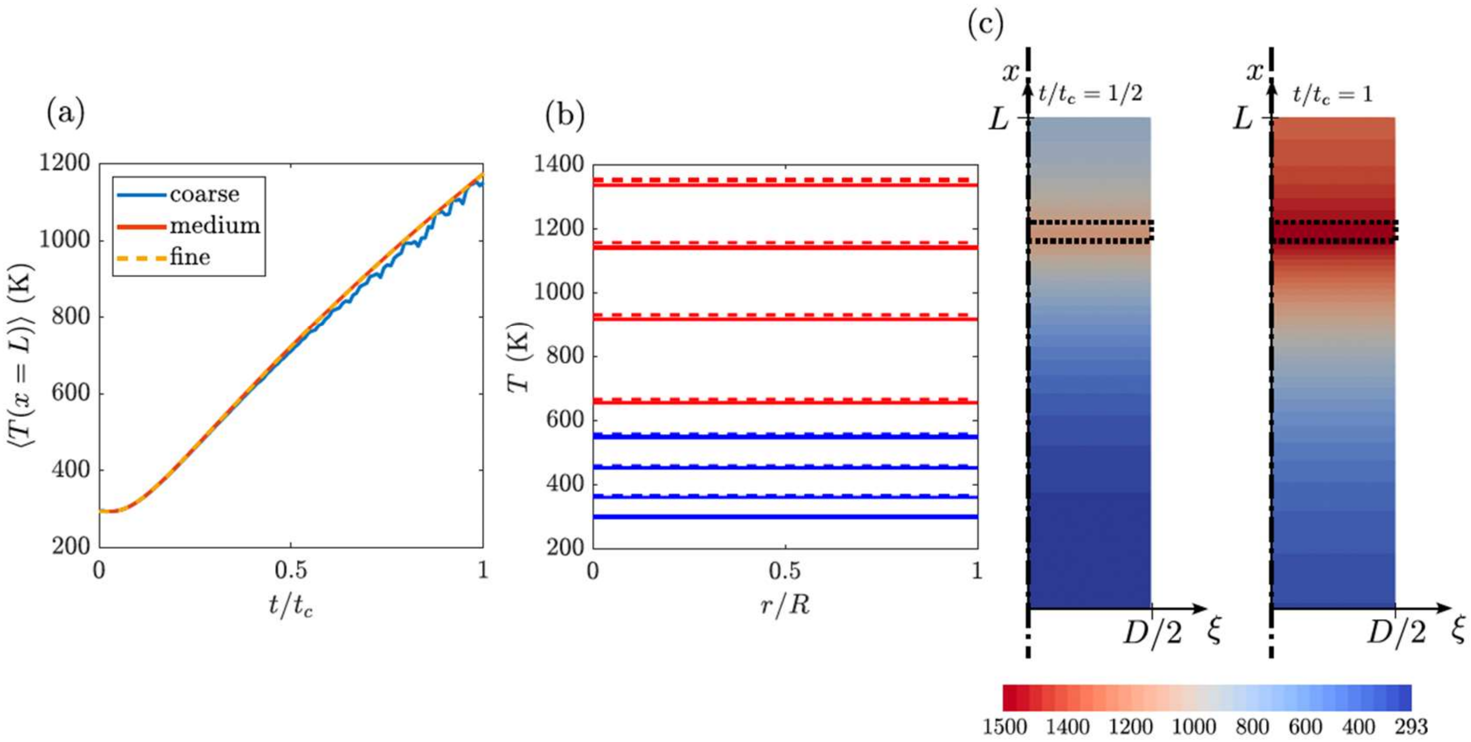

Figure A.1: (a) Mesh sensitivity analysis for the temporal evolution of the spatially-averaged fluid temperature at the tank's outlet; (b) radial profiles of fluid (solid line) and solid (dashed line) temperatures at $x/L = 2/5$ (blue) and $x/L = 3/4$ (red), at the instants $t/t_c = 1/4,\ 1/2,\ 3/4,\ 1$; (c) isocontours of fluid temperature at the times indicated (heat source location is marked with dotted lines). For reference, the results shown in (b) and (c) have been obtained with the medium grid.

$$\varepsilon \frac{\partial \rho}{\partial t} + \nabla \cdot (\rho \mathbf{v}) = 0\,, \tag{A.1}$$

$$\frac{1+(1-\varepsilon)\chi}{\varepsilon^2}\left[\frac{\partial(\rho \mathbf{v})}{\partial t} + \rho \mathbf{v}\cdot\nabla\mathbf{v}\right] = -\nabla p + \rho \mathbf{g} - \left(\frac{\mu}{\Pi} + \frac{\rho F}{2}|\mathbf{v}|\right)\mathbf{v}\,, \tag{A.2}$$

$$\rho C_p\left(\varepsilon \frac{\partial T}{\partial t} + \mathbf{v}\cdot\nabla T_f\right) = \nabla\cdot(\varepsilon k \nabla T) - h_v(T - T_s)\,, \tag{A.3}$$

$$(1-\varepsilon)\rho_s C_s \frac{\partial T_s}{\partial t} = \nabla\cdot[(1-\varepsilon)k_s\nabla T_s] + h_v(T - T_s) + Q(\mathbf{x}, t)\,, \tag{A.4}$$

Results. Design conditions for IH-TESLA

Max. temperatures:

$$\theta_e^{\max} = \frac{1}{2}\left[1 + \operatorname{erf}(m)\right] + \frac{e^{-m^2}}{2\,m\sqrt{\pi}}, \qquad m = \frac{\Lambda\sqrt{\Delta}}{2a}$$

$$\theta_{se}^{\max} = \frac{1}{2}\left[1 + \operatorname{erf}(m_s)\right] + \frac{e^{-m_s^2}}{2\,m_s\sqrt{\pi}}, \qquad m_s = \frac{\Lambda\sqrt{\Delta}}{2(a+1)}$$

Positions:

$$\eta_e^{\max} = \eta_1 + \frac{\Delta}{2\,a\,\epsilon} = \eta_1 + \Lambda\frac{\Delta}{2\,a},$$

$$\eta_{se}^{\max} = \eta_1 + \frac{\Delta}{2(a+1)\epsilon} = \eta_1 + \Lambda\frac{\Delta}{2(a+1)},$$

Main design condition: $\theta = 1$ at $\eta = 1$

Additional constraints:

$\eta_e^{max} \leq 1.$ → $\frac{\gamma\Delta}{\beta\kappa} \leq 2(1-\eta_1).$ Final temperature lies inside the tank

$\theta_{se}^{\max} \leq \theta_e^{\max}$ → $\frac{\Lambda\sqrt{\Delta}}{2(a+1)} \gtrsim 1.$ Avoids solid overheating

Range for practical tank design:

$$\frac{4(a+1)^2}{\Lambda^2} \lesssim \Delta \leq \frac{2(1-\eta_1)a}{\Lambda}$$

Key parameters:

$$\Delta = \frac{\delta}{L} \qquad \Lambda = \frac{h_v L}{\varepsilon\rho C_p u_0} \qquad a = \frac{k_s(1-\varepsilon)\,h_v}{(\varepsilon\rho C_p u_0)^2}$$

a modulates the heat transfer with the conductivities ratio

$$a = \Lambda\beta\frac{k_s(1-\varepsilon)/h_v}{k\varepsilon/h_v} \sim k_s/k$$

Design recommendations and operational conditions for IH-TESLA

Heat source location:

$$\eta_1 = 3/4.$$

Heat source required power:

$$Q(\eta,\tau) = q(\eta,\tau)\frac{\rho C_p \varepsilon u_0 (T_f - T_0)}{L} = \tanh\left(\frac{\tau}{\Delta_\tau}\right)\frac{\exp\left[-(\eta-\eta_1)^2/\Delta\right]}{\sqrt{\pi\Delta}},$$

Heat source thickness:

$$\Delta \equiv \frac{\delta}{L} = (1-\eta_1)\frac{a}{\Lambda} = (1-\eta_1)\frac{\kappa\beta}{\gamma} = (1-\eta_1)\frac{1-\varepsilon}{\varepsilon}\frac{k_s}{L u_0 \rho C_p},$$

Max. HTF temperature location:

$$\eta_e^{max} = (1+\eta_1)/2,$$

Heating time:

$$t_c = \frac{\Delta}{1-\eta_1}\frac{\rho_s C_s}{k_s}L^2 = \frac{\Delta}{1-\eta_1}\frac{L^2}{\alpha_s} = \frac{\delta}{1-\eta_1}\frac{L}{\alpha_s},$$

Case study: Design of IH-TESLA tank filled with randomly-packed spherical particles of alumina, SiC and concrete

Adopted dimensions: $\Delta = 1/50 \quad \eta_1 = 3/4 \quad d_p > 1\ \mathrm{cm}$

$$t_c = \frac{2}{25}\frac{L^2}{\alpha_s},$$

$$\varepsilon = 1 - \frac{2}{25}\frac{GC_pL}{A\,k_s}, \qquad \varepsilon = 0.390 + \frac{1.740}{(D/d_p + 1.140)^2}$$

Porosity correletion for spheres [Benyahia and O'Neill (2005)]

$$\frac{\Delta p}{L} = 150\frac{(1-\varepsilon)^2\nu}{\Phi_s^2\,\varepsilon^3\,d_p^2}\left(\frac{G}{A}\right) + 1.75\frac{(1-\varepsilon)}{\rho\,\Phi_s\,\varepsilon^3\,d_p}\left(\frac{G}{A}\right)^2$$

Ergun's equation [Ergun and Orning (1949)]

Table 4: Summary of design and operation points for an IH-TESLA tank with randomly-packed spherical fillers of various materials, under different power performances at $(\Delta T) \simeq 1000$ K.

	Q (kW)	t_c^* (h)	ε^*	d_p^* (cm)	G^* (g/s)	V_s^* (ℓ)	L^* (m)	D^* (m)	δ^* (cm)	$P^* \times 10^{-5}$ (W)
Alumina	10.0	5.03	0.395	2	0.32	36.33	0.67	0.34	1.35	30.54
SiC	100.0	1.87	0.403	6	3.16	224.11	1.24	0.62	2.48	219.33
Concrete	2.5	8.02	0.397	2	0.08	21.17	0.56	0.28	1.13	2.18

Design results

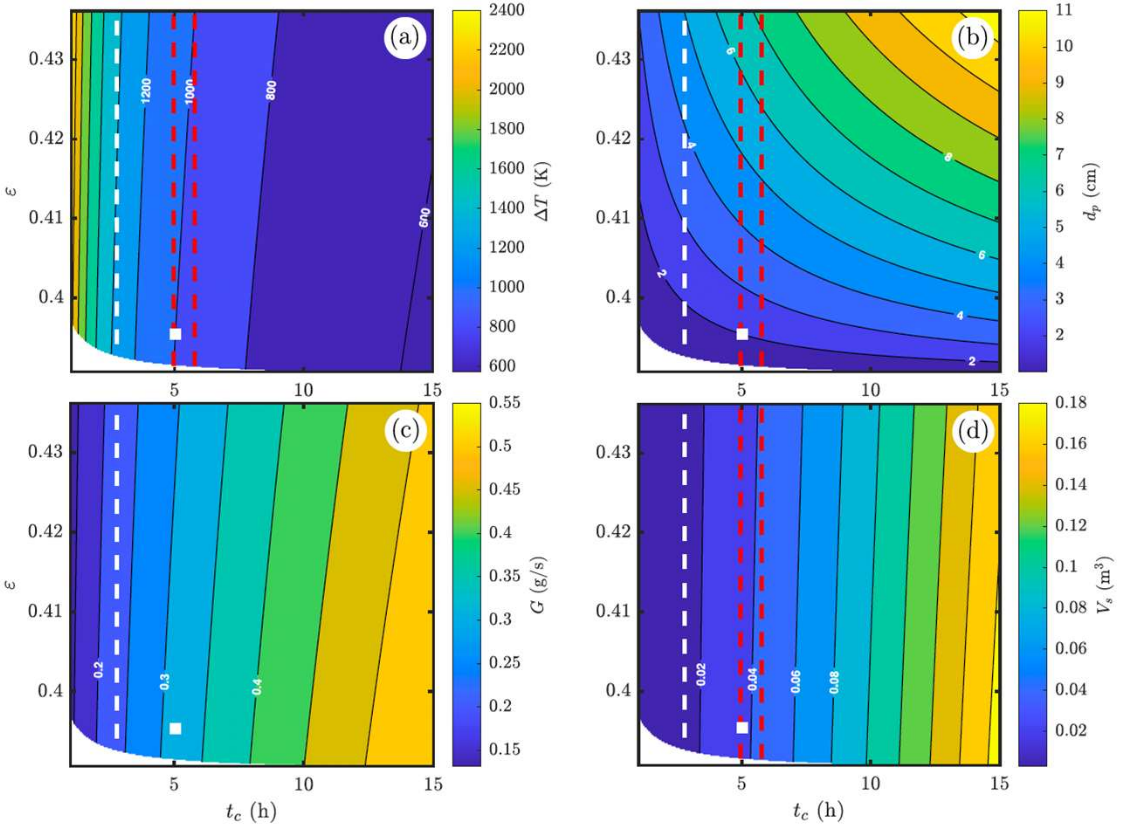

Figure 1: Results for an IH-TESLA tank filled with alumina spherical particles at $Q = 10$ kW. From (a) to (d): Evolutions of temperature drop, particle size, mass-flow rate, and volume of fillers, with the tank porosity and with the heating time. The white-square marker represents the design point (t_c^*, ε^*). The dashed-white line indicates the minimum heating time ($t_{c\,\mathrm{min}} = 2.77$ h) that can be reached in view of Eq. (14), assumed $\delta_0 = 1$ cm. The region delimited by the two red dashed lines indicates t_c range for which $\langle \Delta T \rangle = 1000$ K is met. The blank region removes the area $d_p < 1$ cm.

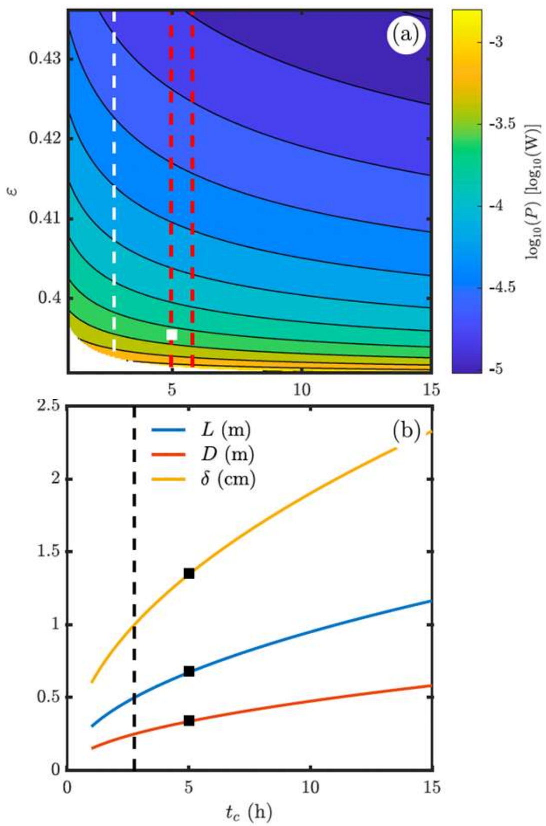

ǯa

Conclusions and future works (I)

1. Development Theoretical Framework:

- Analytical approximate solution for **Internally-Heated TES** with localized heat source **(IH-TESLA)**
- Dimensionless parameters: Λ , κ , β , γ , η_1 , Δ

2. Asymptotic Analytical Solutions:

Validated against simulations.

Predicts:

- **Transient time until final state**
- **Temperature profiles** (fluid + solid)
- **Max temperature positions & magnitudes**

Conclusions and future works (II)

3. Practical Design Guidelines

- Heat source location & thickness
- Charging time
- Risk of overheating in solids
- Outlet temperature performance

4. Engineering Impact

Results provide:

- **Quick predictive tools** for IH-TES design.
- **Avoid trial-and-error** design processes.

TO DO:

Enable integration with **renewables & cyclic/dynamic operation (inlet/outlet)**.
Explore simultaneous charge and operation.

Thanks for your attention!

Questions?

Back-up

Summary of existing-TES governing parameters

Ref.	Re	Λ	β	γ	κ	Λ^{-1}	a	Bi
[19]	200.02	3.01	8.68×10^{-4}	3.41×10^{-4}	3.20×10^{-2}	3.32×10^{-1}	2.46×10^{-1}	1.222
[11]	21.92	54.78	3.78×10^{-4}	2.09×10^{-4}	6.22×10^{-3}	1.83×10^{-2}	6.15×10^{-1}	0.081
[11]	109.62	16.12	3.78×10^{-4}	2.09×10^{-4}	6.22×10^{-3}	6.20×10^{-2}	1.81×10^{-1}	0.598
[33]	18.23	2.23	8.88×10^{-4}	1.48×10^{-4}	1.00×10^{-3}	4.49×10^{-1}	1.34×10^{-2}	0.006
[33]	273.48	1.16	5.92×10^{-5}	1.48×10^{-4}	1.00×10^{-3}	8.60×10^{-1}	4.65×10^{-4}	0.044
[45]	276.24	21.91	8.76×10^{-5}	1.10×10^{-4}	7.14×10^{-3}	4.56×10^{-2}	1.07×10^{-1}	0.179
[30]	17628.21	13.62	1.00×10^{-6}	4.34×10^{-3}	7.81×10^{-2}	7.34×10^{-2}	2.45×10^{-4}	19.712
[10]	12.43	41.07	1.91×10^{-3}	1.10×10^{-4}	1.37×10^{-3}	2.44×10^{-2}	9.71×10^{-1}	0.077
[10]	5248.62	60.01	1.62×10^{-6}	7.10×10^{-5}	9.18×10^{-2}	1.67×10^{-2}	1.25×10^{-1}	0.163
[49]	5931.83	97.12	9.80×10^{-7}	9.25×10^{-5}	7.09×10^{-3}	1.03×10^{-2}	7.29×10^{-3}	3.450
[48]	797.54	3.69	3.90×10^{-4}	4.28×10^{-5}	4.48×10^{-1}	2.71×10^{-1}	15.07	0.004
[48]	5021.57	2.37	6.19×10^{-5}	4.28×10^{-5}	4.48×10^{-1}	4.22×10^{-1}	1.54	0.016
[43]	151.26	10.11	1.83×10^{-4}	4.14×10^{-4}	7.46×10^{-3}	9.89×10^{-2}	3.33×10^{-2}	0.568
[35]	785.86	41.36	1.34×10^{-5}	2.35×10^{-4}	3.16×10^{-2}	2.42×10^{-2}	7.45×10^{-2}	0.617
[35]	214.58	31.93	9.90×10^{-5}	1.34×10^{-4}	4.43×10^{-2}	3.13×10^{-2}	1.05	0.025
[27]	4785.34	118.65	5.50×10^{-7}	4.10×10^{-4}	3.37×10^{-2}	8.43×10^{-3}	5.37×10^{-3}	0.842

Table 1: Corresponding values of the parameters (11) for similar works studying air-solid packed-bed IH-TES.

DNS validation with experiments

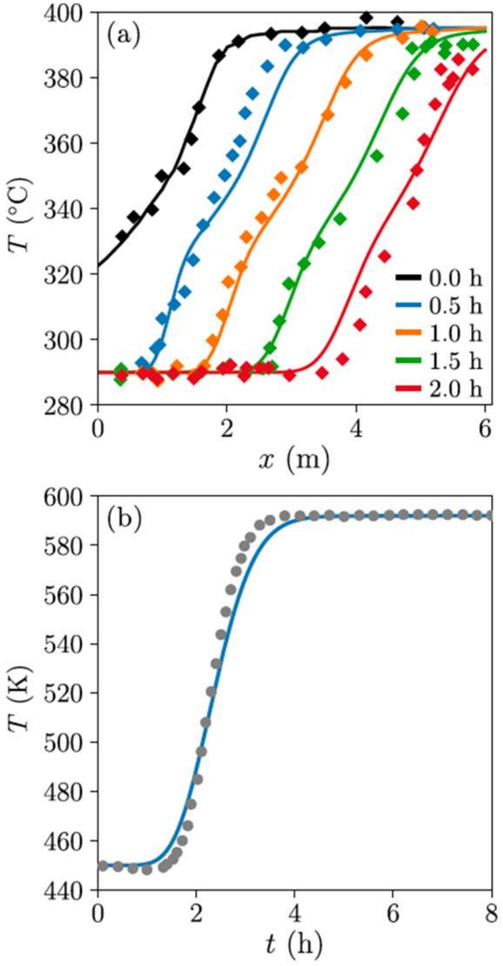

Table A.2: Thermophysical properties of the HTF and of the packed bed material (temperatures in K where needed). Solar salt and quartzite rocks properties are used in Fig. A.1(a), and air and rock in (b).

(a) Solar salt	ρ_f	kg m^{-3}	$2090 - 0.636\,T$
	C_{pf}	J kg^{-1} K^{-1}	$1443 + 0.172\,T$
	k_f	W m^{-1} K^{-1}	$0.443 + 1.9 \times 10^{-4}\,T$
	μ_f	Pa s	$(22.174 - 0.12\,T + 2.281 \times 10^{-4}\,T^2$ $-1.471 \times 10^{-7}\,T^3)/1000$
(a) Quartzite rocks	ρ_s	kg m^{-3}	2640
	C_{ps}	J kg^{-1} K^{-1}	1050
	k_s	W m^{-1} K^{-1}	2.5
(b) Compressed air	ρ_a	kg m^{-3}	15.40
(2×10^6 Pa)	C_{pa}	J kg^{-1} K^{-1}	1039
	k_a	W m^{-1} K^{-1}	0.040
	μ_a	Pa s	2.73×10^{-5}
(b) Rock	ρ_r	kg m^{-3}	2560
	C_{pr}	J kg^{-1} K^{-1}	960
	k_r	W m^{-1} K^{-1}	0.48

Design inputs

Particle shape	Correlation	Range of particle size	Range of porosity	MCC	SE
Spheres	$0.390 + \frac{1.740}{(D/d_p + 1.140)^2}$	$0.02 \leq d_p/D \leq 0.67$	$0.390 \leq \varepsilon \leq 0.63$	0.93	0.015
Solid cylinders	$0.373 + \frac{1.703}{(D/d_p + 0.611)^2}$	$0.04 \leq d_p/D \leq 0.59$	$0.373 \leq \varepsilon \leq 0.69$	0.96	0.016
Hollow cylinders	$0.465 + \frac{2.030}{(D/d_p + 1.033)^2}$	$0.07 \leq d_p/D \leq 0.53$	$0.465 \leq \varepsilon \leq 0.70$	0.92	0.020
4-hole cylinders	$0.595 + \frac{2.082}{(D/d_p + 1.244)^2}$	$0.12 \leq d_p/D \leq 0.53$	$0.595 \leq \varepsilon \leq 0.80$	0.91	0.024

Table 1: Mean porosity correlations, and d_p/D and ε validity ranges for the considered particle shapes (adapted from Benyahia and O'Neill [33]; MCC is the Multiple Correlation Coefficient and SE the Standard Error).

Table 2: Thermophysical properties of the packed-bed fillers at 500 °C.

	C_s (J/kg K)	k_s (W/m K)	ρ_s (kg/m^3)
Alumina [30]	1250	10	3987
SiC [30]	900	55	3160
Concrete [42]	1100	3	3100

Design costs

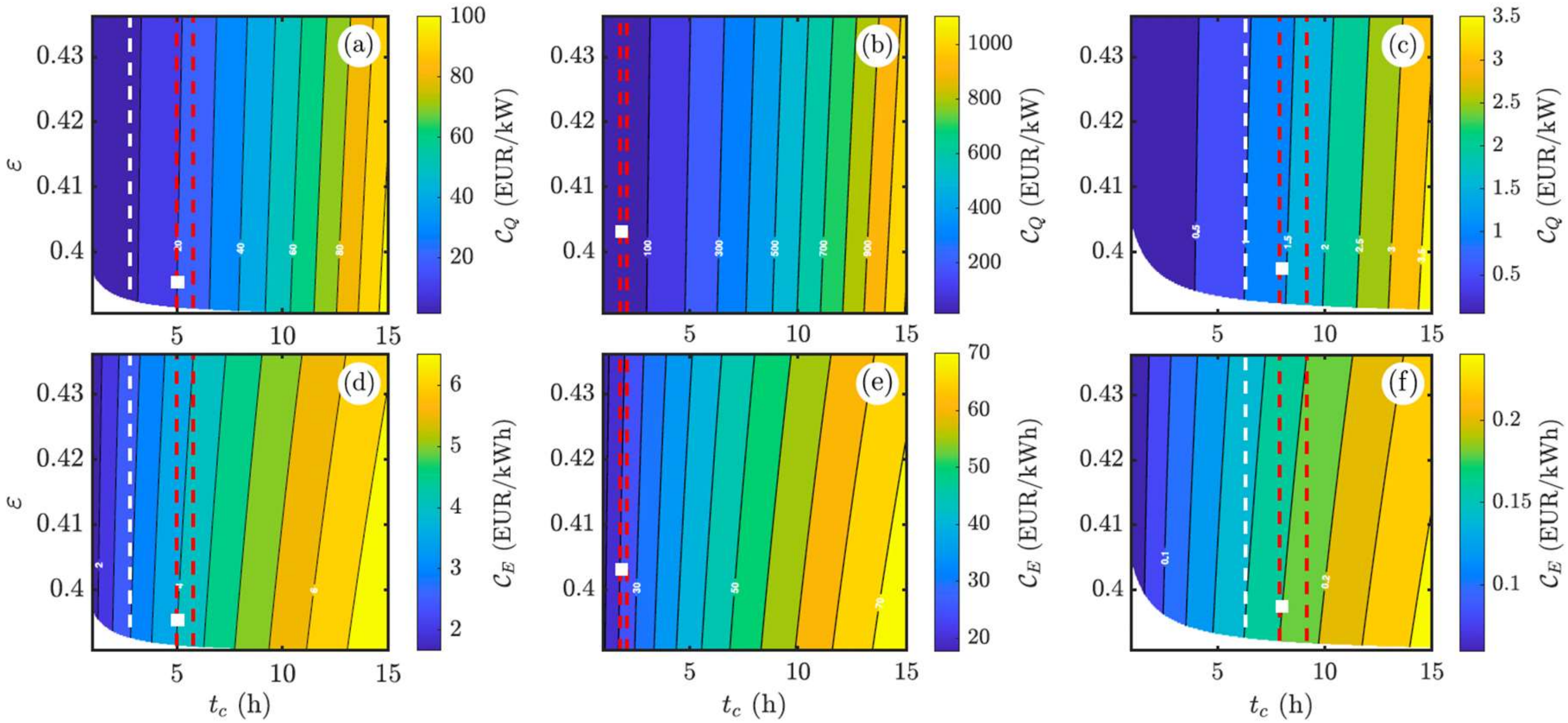

Table C.1: Costs per unit power ($\mathcal{C}_Q$) and per unit energy ($\mathcal{C}_E$) for randomly-packed spherical particles of alumina, SiC, and concrete, at design and operation points at $\langle \Delta T \rangle \simeq 1000$ K (from Table 4).

	Q (kW)	t_c^* (h)	V_s^* (ℓ)	$\mathcal{P}^*$ (EUR/kg) [45]	$\mathcal{C}_Q^*$ (EUR/kW)	$\mathcal{C}_E^*$ (EUR/kWh)
Alumina	10.0	5.03	36.33	1.39	20.27	4.03
SiC	100.0	1.87	224.11	4.50 - 9.00	31.85 - 63.77	17.03 - 34.10
Concrete	2.5	8.02	21.17	0.03 - 0.08	0.80 - 2.08	0.10 - 0.26